

A 0.4-mm-diameter probe for nonlinear optical imaging

Hongchun Bao and Min Gu*

Centre for Micro-Photonics, Faculty of Engineering & Industrial Sciences, Swinburne University of Technology,
Hawthorn, Victoria 3122, Australia
mgu@swin.edu.au

Abstract: A miniaturized probe that possesses a diameter of 0.4 mm is developed for two-photon-excited fluorescence imaging. The miniaturized probe was manufactured by the collapse of air holes and the formation of a lens on the tip of a double-clad photonic crystal fiber (DCPCF) using electric arc discharging from a conventional fusion splicer. As a result, a femtosecond pulsed laser beam delivered by the DCPCF can be directly focused on a sample for two-photon fluorescence imaging. The numerical aperture of the lensed DCPCF is 0.12. The corresponding focal spot size is 6 μm , which is close to the diffraction limit. This 0.4-mm-diameter probe can provide clear two-photon-excited fluorescence images of 10- μm -diameter fluorescent microspheres.

©2009 Optical Society of America

OCIS codes: (110.2350) Fiber optical imaging; (180.4315) Nonlinear microscopy; (110.3080) Infrared imaging; (110.6880) Three-dimensional image acquisition; (170.2150) Endoscopic imaging.

References and links

1. W. Denk, J. H. Strickler, and W. W. Webb, "Two-photon laser scanning fluorescence microscopy," *Science* **248**(4951), 73–76 (1990).
2. H. Bao, J. Allen, R. Pattie, R. Vance, and M. Gu, "Fast handheld two-photon fluorescence microendoscope with a 475 microm x 475 microm field of view for in vivo imaging," *Opt. Lett.* **33**(12), 1333–1335 (2008).
3. B. A. Flusberg, J. C. Jung, E. D. Cocker, E. P. Anderson, and M. J. Schnitzer, "*In vivo* brain imaging using a portable 3.9 gram two-photon fluorescence microendoscope," *Opt. Lett.* **30**(17), 2272–2274 (2005).
4. K. König, A. Ehlers, I. Riemann, S. Schenkl, R. Bückle, and M. Kaatz, "Clinical two-photon microendoscopy," *Microsc. Res. Tech.* **70**(5), 398–402 (2007).
5. T. P. Thomas, J. Y. Ye, Y. C. Chang, A. Kotlyar, Z. Cao, I. J. Majoros, T. B. Norris, and J. R. Baker, Jr., "Investigation of tumor cell targeting of a dendrimer nanoparticle using a double-clad optical fiber probe," *J. Biomed. Opt.* **13**(1), 014024 (2008).
6. D. Bird, and M. Gu, "Compact two-photon fluorescence microscope based on a single-mode fiber coupler," *Opt. Lett.* **27**(12), 1031–1033 (2002).
7. D. Bird, and M. Gu, "Two-photon fluorescence endoscopy with a micro-optic scanning head," *Opt. Lett.* **28**(17), 1552–1554 (2003).
8. D. Bird, and M. Gu, "Fibre-optic two-photon scanning fluorescence microscopy," *J. Microsc.* **208**(1), 35–48 (2002).
9. L. Fu, X. Gan, and M. Gu, "Use of a single-mode fiber coupler for second-harmonic-generation microscopy," *Opt. Lett.* **30**(4), 385–387 (2005).
10. F. Helmchen, M. S. Fee, D. W. Tank, and W. Denk, "A miniature head-mounted two-photon microscope. high-resolution brain imaging in freely moving animals," *Neuron* **31**(6), 903–912 (2001).
11. M. T. Myaing, D. J. MacDonald, and X. Li, "Fiber-optic scanning two-photon fluorescence endoscope," *Opt. Lett.* **31**(8), 1076–1078 (2006).
12. L. Fu, X. Gan, and M. Gu, "Nonlinear optical microscopy based on double-clad photonic crystal fibers," *Opt. Express* **13**(14), 5528 (2005).
13. L. Fu, A. Jain, H. Xie, C. Cranfield, and M. Gu, "Nonlinear optical endoscopy based on a double-clad photonic crystal fiber and a MEMS mirror," *Opt. Express* **14**(3), 1027–1032 (2006).
14. L. Fu, and M. Gu, "Double-clad photonic crystal fiber coupler for compact nonlinear optical microscopy imaging," *Opt. Lett.* **31**(10), 1471–1473 (2006).
15. L. Fu, A. Jain, C. Cranfield, H. Xie, and M. Gu, "Three-dimensional nonlinear optical endoscopy," *J. Biomed. Opt.* **12**(4), 040501 (2007).

16. M. T. Myaing, J. Y. Ye, T. B. Norris, T. Thomas, J. R. Baker, Jr., W. J. Wadsworth, G. Bouwmans, J. C. Knight, and P. S. Russell, "Enhanced two-photon biosensing with double-clad photonic crystal fibers," *Opt. Lett.* **28**(14), 1224–1226 (2003).
17. L. Fu, and M. Gu, "Fibre-optic nonlinear optical microscopy and endoscopy," *J. Microsc.* **226**(3), 195–206 (2007).
18. C. L. Hoy, N. J. Durr, P. Chen, W. Piyawattanametha, H. Ra, O. Solgaard, and A. Ben-Yakar, "Miniaturized probe for femtosecond laser microsurgery and two-photon imaging," *Opt. Express* **16**(13), 9996–10005 (2008).
19. D. Yelin, I. Rizvi, W. M. White, J. T. Motz, T. Hasan, B. E. Bouma, and G. J. Tearney, "Three-dimensional miniature endoscopy," *Nature* **443**(7113), 765 (2006).
20. T. P. Thomas, J. Y. Ye, C. Yang, M. Myaing, I. J. Majoros, A. Kotlyar, Z. Cao, T. B. Norris, and R. James, "Baker Jr, "Tissue distribution and real-time fluorescence measurement of a tumor-targeted nanodevice by a two photon optical fiber fluorescence probe," *Proc. SPIE* **6095**, 60950Q (2006).
21. C. J. Engelbrecht, R. S. Johnston, E. J. Seibel, and F. Helmchen, "Ultra-compact fiber-optic two-photon microscope for functional fluorescence imaging *in vivo*," *Opt. Express* **16**(8), 5556–5564 (2008).
22. G. J. Kong, J. Kim, H. Y. Choi, J. E. Im, B. H. Park, U. C. Paek, and B. H. Lee, "Lensed photonic crystal fiber obtained by use of an arc discharge," *Opt. Lett.* **31**(7), 894–896 (2006).
23. H. Bao, and M. Gu, "Reduction of self-phase modulation in double-clad photonic crystal fiber for nonlinear optical endoscopy," *Opt. Lett.* **34**(2), 148–150 (2009).
24. N. Mihajlovic, G.W. 't Hooft, B.H.W. Hendriks, W.C.J. Bierhoff, C.A. Hezemans, R. Harbers, A.L. Braun, J.J.L. Horikx, and A.E. Desjardins, "Electromagnetically-Controlled Fiber-Scanning Confocal Microscope," OSA Optics & Photonics Congress, NWC5, (2009).

1. Introduction

Nonlinear optical microscopy based on multi-photon-excited fluorescence uses a near infrared laser beam for imaging, which could identify cell structures of tissue deep beneath the surface [1–3]. However, despite of its usefulness, nonlinear microscopy imaging using a standard laboratory microscopy with inflexible free-space light delivery limits its applications especially for clinical or animal studies. A flexible fiber-optical probe is versatile to deliver light into tight space where free-space delivery is difficult [4,5]. So far, three different types of fiber have been adopted for multi-photon-excited fluorescence imaging. Single-mode fiber was first used for this purpose [6–10] but such a system exhibits a low signal level because the near infrared laser beam and the visible fluorescence signal cannot efficiently propagate through the core of the fiber [8]. This issue has been overcome by using a double-clad fiber [2,11]. In fact, the signal level can be further increased when a double-clad photonic crystal fiber (DCPCF) that has a large core is applied [12–17]. In all these micro-probe designs, coupling optics has been used to deliver the excitation beam and collect fluorescence, which eventually leads to a probe size over 1.5 mm [2,10,18].

Reducing the size of probes is essential for minimizing invasion during medical procedures and reducing the risk of complications as well as costs and recovery times [19–21]. In this paper, we demonstrate a small probe with a diameter of 0.4 mm, which is only one third of the size of a normal micro-probe [15]. The 0.4-mm-diameter probe is developed by the formation of a semi-sphere lens on the tip of a DCPCF which is used for delivering a femtosecond pulsed laser beam to samples and collecting the two-photon fluorescence signal for imaging. The 0.4-mm-probe can produce a diffraction-limited focal spot with a full width at half-maximum (FWHM) of 6 μm and thus provide clear images of 10 μm fluorescent microspheres.

2. Two-photon-excited fluorescence imaging system

Figure 1 is the schematic setup for two-photon-excited fluorescence imaging using the 0.4-mm-diameter optical probe. A DCPCF is used to deliver 80 MHz repetition rate pulses of 100 fs from a Ti:Sapphire laser to a sample to excite two-photon fluorescence signal. The excitation laser beam has a center wavelength of 800 nm with a FWHM bandwidth of 12 nm. In order to keep a short pulse width, a prechirp unit – a grating pair is used to implement negative frequency chirping to the pulses from the Ti:Sapphire laser [2], so that the chromatic dispersion of the DCPCF is compensated. The schematic structure of the DCPCF is displayed in the low left corner of Fig. 1. The solid core of the DCPCF, which is in the center of the

DCPCF, has a diameter of 16 μm and is surrounded by a hexagon array of air holes. The hexagon is surrounded by air holes arrayed in a ring. Inside the ring, the inner-cladding of the DCPCF has a diameter of 160 μm , where the outer-cladding of the DCPCF is the part of the fiber outside of the ring, having a diameter of 350 μm .

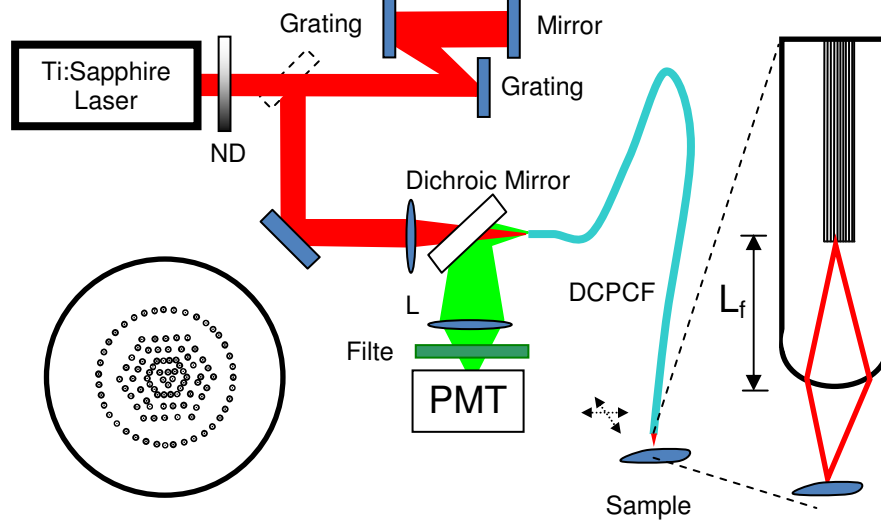


Fig. 1. Schematic setup for two-photon-excited fluorescence imaging using a 0.4-mm-diameter optical fiber probe.

The enlarged structure of the end of the DCPCF is shown in the right of Fig. 1. The tip of the DCPCF is shaped into a semi-sphere by applying electric arc discharges on the DCPCF using a conventional fusion splicer [22]. The electric arc discharges melt the tip of the DCPCF and then the tip is gradually developed into a semi-sphere shape. As shown in the enlarged DCPCF tip in Fig. 1, there is a length of the air-hole collapsed region of L_f . This region in the DCPCF is also developed by applying electric arc discharges on the DCPCF using the conventional fusion splicer [22]. The length L_f can be varied by changing the length of the region where the electric arc discharges are applied. The region of the collapsed air holes in the DCPCF is used for the expansion of the excitation laser beam. The expanded excitation laser beam is then focused on a sample by the lens on the tip the DCPCF, as shown in the inset of Fig. 1. The two-photon-excited fluorescence signal from the sample is collected by the lens and the inner-clad region of the DCPCF, separated from the excitation laser beam by a dichroic mirror and sent into a photomultiplier tube (PMT) after being filtered by a 3 mm thick BG18 glass filter for imaging.

3. 0.4-mm-diameter optical fiber probe

The size of the focal spot by the optical fiber probe is determined by the length of L_f and the shape of the lens on the tip of the DCPCF. The radius of the lens can be adjusted by changing the number of times of the electric arc discharges applied to the fiber tip. Figure 2 shows the simulation and experiment results of the full width at half-maximum of the focal spot, the numerical aperture (NA) and the working distance of the DCPCF tip as a function of L_f while the radius (R) of the semi-sphere on the tip of the DCPCF is 200 μm , 250 μm , and 300 μm , respectively. The simulation result was obtained using commercial lens design software (ZEMAX 2008). From Fig. 2(a), we can see that the focal spot size decreases with the increase of L_f when $L_f < 2.4$ mm. In that region, the NA of the probe is small as shown in Fig. 2(b) and the corresponding focal spot is diffraction limited. From Fig. 2(b), we can see that the increase of L_f leads to the increase of NA. The diffraction limited focal spot size is inversely proportional to the NA of the lensed tip and therefore it reduces with the increase of

L_f . As L_f reaches 2.4 mm, 2.8 mm, and 3.2 mm as displayed in Fig. 2(a), the FWHM of the focal spot approaches the minimum values of 5.42 μm , 6 μm and 6.21 μm when the radius of the DCPCF tip is 200 μm , 250 μm , and 300 μm , respectively.

A further increase of L_f results in the decrease of the focal spot size because the focus spot is not diffraction limited. In this region, an increase of L_f leads to the increase of the expansion of the excitation beam though the corresponding NA of the lensed tip is enlarged. However spherical aberration of the lens, caused by the large beam expansion, increases rapidly and the resultant focal spot is no longer diffraction limited. The focal spot size increases as a result of the increase of the spherical aberration of the lens. Figure 2(a) and Fig. 2(b) also show the experimentally measured focal spot size and NA versus L_f for $R = 200 \mu\text{m}$. The simulation results agree well with the experiment measurement. Figure 2(c) displays the working distance of the DCPCF lensed tip. The working distance decreases with the increase of L_f . For $R = 200 \mu\text{m}$ and $L_f = 2.4 \text{ mm}$, while the focal spot size of the DCPCF tip is minimum, the working distance of the DCPCF tip is 0.5 mm.

The images of the manufactured DCPCF tips and the corresponding focal spots are revealed in Fig. 3. Figure 3(a) and Fig. 3(c) are the optical microscopy transmission images of the DCPCF tips with $L_f = 1.4 \text{ mm}$ and 2.4 mm, respectively. At the top of the DCPCF, a smooth semi-sphere is formed. The radius of the semi-spheres is 200 μm . This semi-sphere tip is used as a lens. The region where the DCPCF shows the bright strip in the middle is the place where the collapse of air holes occurs. This region is used for the expansion of the excitation laser beam. Figure 3(b) and Fig. 3(d) are the charge coupled device (CCD, Watec WAT-902H) records of the light intensity images of the focal spot taken at the end of the DCPCF tips (a) and (c), respectively. The measured FWHM of the laser focal spot in Fig. 2 was measured from the light intensity images recorded by the CCD camera.

The DCPCF tip as shown in Fig. 3(c) is used as a micro-probe for two-photon excited fluorescence imaging. The images were currently obtained by scanning the sample. If a micro-scanner was employed, the images could be obtained by scanning the micro-probe [24]. Figure 4 is a set of two-photon-excited fluorescence images of 10- μm -diameter fluorescent microspheres, taken by this 0.4-mm-diameter optical probe. The illumination power on the sample is 10 mW and the input power to the optical fiber probe is 34 mW. The coupling ratio, which is the ratio of the output power to the input power, of the optical DCPCF probe is 29%. The coupling efficiency of a DCPCF is 82% [23]. However only 38% of the coupling light is in the core of the DCPCF and the rest is at the inner-cladding [23]. The NA of the core and inner cladding of the DCPCF is 0.04 and 0.62 respectively [23]. The low NA beam from the core of the DCPCF can effectively be focused by the lens on the tip of the DCPCF, while most of the high NA beam from the inner cladding exits the DCPCF before it reaches the lens. Therefore the focused laser mainly comes from the core of the DCPCF, which is useful for the generation of fluorescence signal [23]. The coupling ratio of the DCPCF probe is close to the coupling efficiency of a DCPCF in the core. Therefore, the loss introduced by the collapse of air holes and the formation of the lens is small and can be neglected. In addition, the chromatic dispersion of the DCPCF probe is the same as that of the DCPCF with the same length. Therefore, the chromatic dispersion from the lens of the DCPCF is much lower than that from the DCPCF and can be neglected.

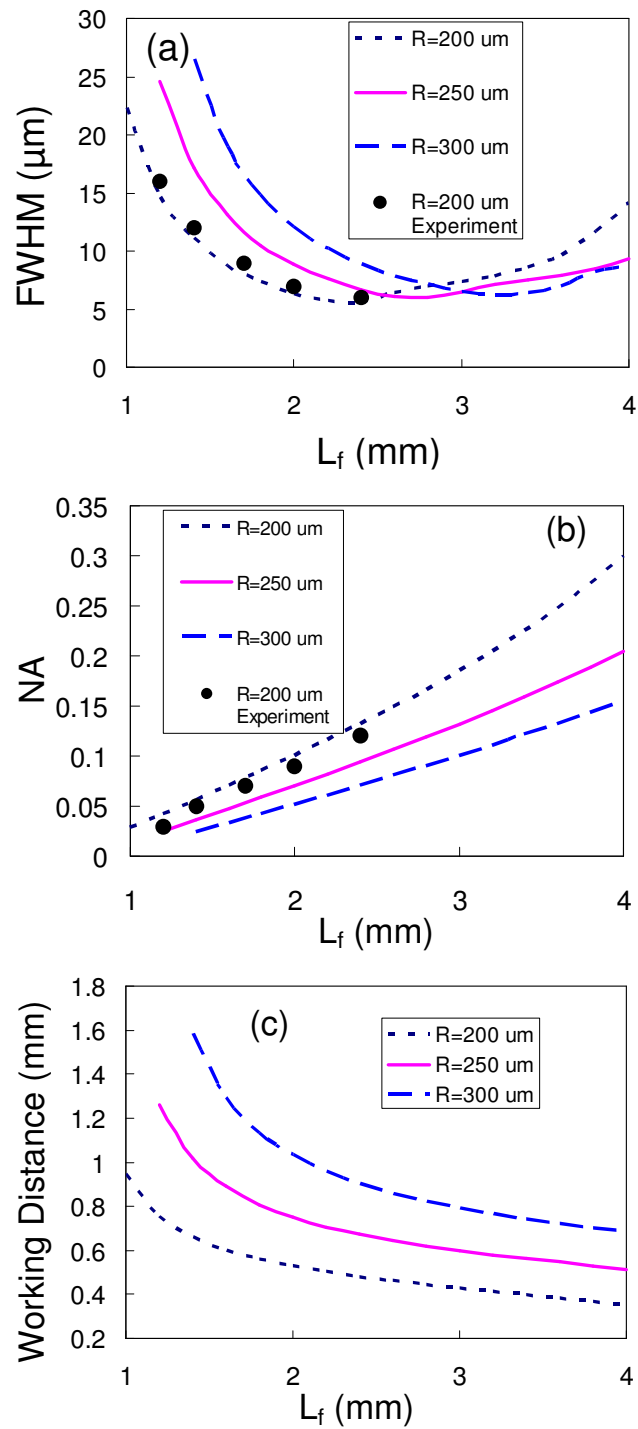


Fig. 2. (a) FWHM of the excitation laser focal spot, (b) NA of the DCPCF lens and (c) working distance of the DCPCF lens tip versus L_f while the radius (R) of the DCPCF lens tip is 200 μm , 250 μm , and 300 μm , respectively.

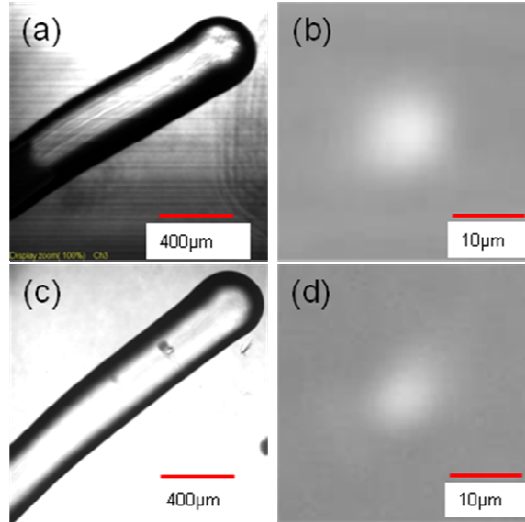


Fig. 3. (a) Optical microscopy transmission image of the fabricated DCPCF tip with $R = 200 \mu\text{m}$ and $L_f = 1.4 \text{ mm}$. (b) Light intensity image of the excitation laser focal spot using the DCPCF tip in (a). (c) Optical microscope transmission image of the fabricated DCPCF tip with $R = 200 \mu\text{m}$ and $L_f = 2.4 \text{ mm}$. (d) Light intensity image of the excitation laser focal spot using the DCPCF tip in (c).

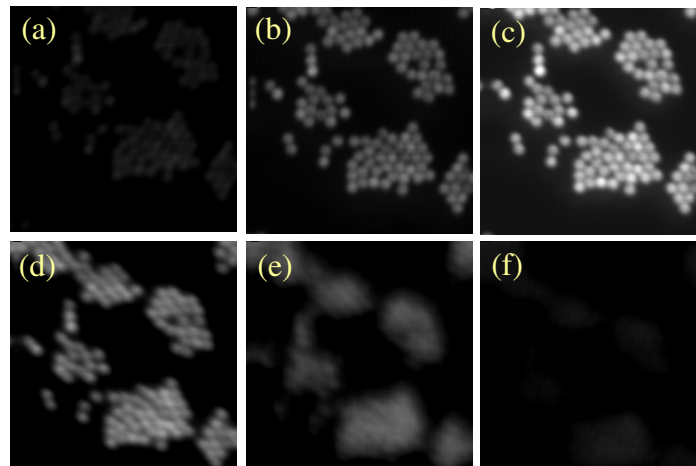


Fig. 4. A set of two-photon-excited fluorescence images of $10\text{-}\mu\text{m}$ -diameter fluorescent microspheres. Size of the images: $200 \mu\text{m} \times 200 \mu\text{m}$. (a) $D = 530 \mu\text{m}$ (b) $D = 490 \mu\text{m}$ (c) $D = 450 \mu\text{m}$ (d) $D = 410 \mu\text{m}$ (e) $D = 370 \mu\text{m}$ (f) $D = 330 \mu\text{m}$.

The two-photon fluorescence images of $10\text{-}\mu\text{m}$ -diameter fluorescent microspheres at different D , where D is the distance between the surface of the DCPCF probe and $10\text{-}\mu\text{m}$ -diameter fluorescent microspheres, are shown in Figs. 4(a)-(f). Figure 4(c) displays clear and bright two-photon-excited fluorescence image of the $10 \mu\text{m}$ fluorescent microspheres. Therefore the working distance of the probe is 0.45 mm , which is close to the simulation results as illustrated in Fig. 2(c). The measured collection efficiency of fluorescence signal with $\text{NA} = 0.12$ is 68% . The DCPCF probe has high signal collection efficiency of two-photon-excited fluorescence signal.

4. Conclusions

In summary, a miniaturized optical fiber probe of 0.4 mm in diameter has been demonstrated. A micro-lens of NA up to 0.12 has been directly formed at the end of a DCPFC so that no extra-coupling optics is needed for simultaneous two-photon fluorescence excitation and collection. Clear two-photon-excited fluorescence imaging of 10 μm fluorescent microspheres has been obtained in this 0.4-mm-diameter system. Such a light and rigid probe may be advantageous for future *in vivo* nonlinear optical endoscopy [2,24].

Acknowledgements

The authors thank the Australian Research Council for its support and Optiscan Pty. Ltd. for providing ZEMAX 2008.